LBL-25085
Preprint

Center for Advanced Materials

CAM

Submitted to Surface Science

DEC 2 1988

Carbon Monoxide Induced Ordering of Adsorbates on the Rh(111) Crystal Surface: Importance of Surface Dipole Moments

C.M. Mate, C.-T. Kao, and G.A. Somorjai

April 1988

TWO-WEEK LOAN COPY

This is a Library Circulating Copy which may be borrowed for two weeks.

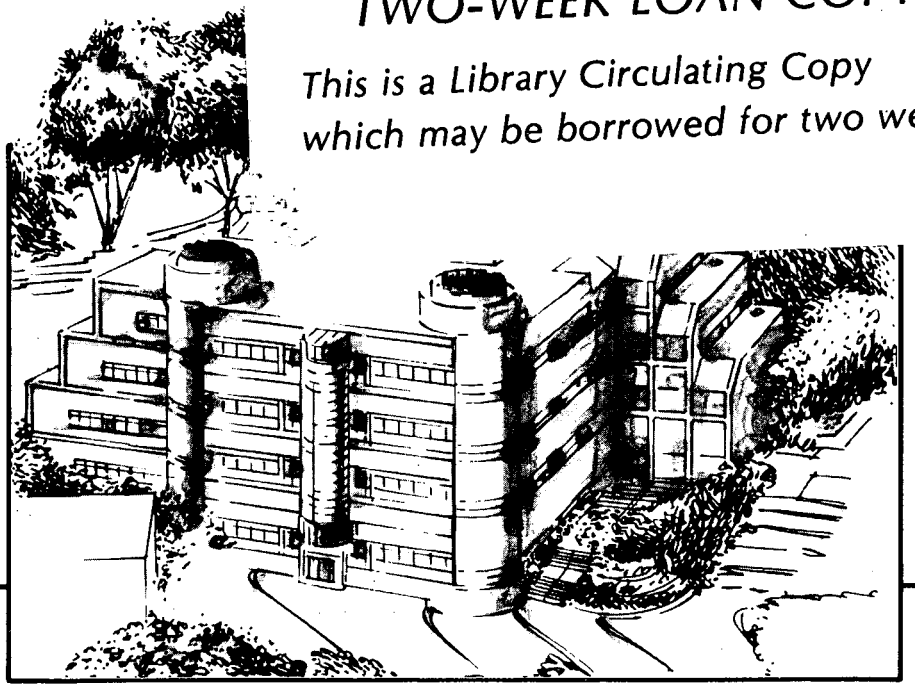

Materials and Chemical Sciences Division

Lawrence Berkeley Laboratory • University of California

ONE CYCLOTRON ROAD, BERKELEY, CA 94720 • (415) 486-4755

Prepared for the U.S. Department of Energy under Contract DE-AC03-76SF00098

LBL-25085 c.2

DISCLAIMER

This document was prepared as an account of work sponsored by the United States Government. While this document is believed to contain correct information, neither the United States Government nor any agency thereof, nor the Regents of the University of California, nor any of their employees, makes any warranty, express or implied, or assumes any legal responsibility for the accuracy, completeness, or usefulness of any information, apparatus, product, or process disclosed, or represents that its use would not infringe privately owned rights. Reference herein to any specific commercial product, process, or service by its trade name, trademark, manufacturer, or otherwise, does not necessarily constitute or imply its endorsement, recommendation, or favoring by the United States Government or any agency thereof, or the Regents of the University of California. The views and opinions of authors expressed herein do not necessarily state or reflect those of the United States Government or any agency thereof or the Regents of the University of California.

Carbon Monoxide Induced Ordering of Adsorbates on the Rh(111) Crystal Surface: Importance of Surface Dipole Moments

C. Mathew Mate*, Chi-Tzu Kao, and Gabor A. Somorjai

Materials and Chemical Sciences Division
Lawrence Berkeley Laboratory
and the Department of Chemistry
University of California
Berkeley, California 94720

*Permanent address: IBM Almaden Research Center,
San Jose, CA 95120

Abstract

To better understand why carbon monoxide induces order in many adsorbed overlayers on metal surfaces, we have measured, from work function changes, the surface dipole moments on Rh(111) for adsorbed CO and for several coadsorbates - sodium, benzene, fluorobenzene, and ethylidyne - which form ordered, coadsorbed structures with CO on the Rh(111) surface. We find that those adsorbates with a positive surface dipole moment form ordered structures when coadsorbed with CO, which is determined to have a negative surface dipole moment. It is proposed that coadsorbing oppositely oriented dipoles strongly promotes the formation of ordered coadsorbed structures. Further, we find that the reduction of the C-O stretching frequency of coadsorbed CO is correlated to the magnitude of the dipole moment of the coadsorbates. This correlation is discussed in terms of the combination of various interactions.

1. Introduction

An understanding of the interactions between different chemical species coadsorbed on surfaces should be an important part of a molecular scale understanding of many surface phenomena. Recently, we reported that carbon monoxide induces order in adsorbed benzene overlayers on Rh(111) and Pt(111) surfaces [1]. Since that initial report, carbon monoxide induced ordering has also been observed for a wide variety of adsorbates {acetylene [2] [3] [4] , ethylidyne ($\equiv CCH_3$) [2] [4] [5] [6] , propylidyne ($\equiv CHCH_2CH_3$) [2] [4] [7] , benzene [4] [6] [8] [9] [10] [11] , fluorobenzene [2] [4] , sodium [2] [4] , potassium [12] [13] , and hydrogen [14]} on several metal surfaces {Rh(111) [1-5,7-9], Pt(111) [1] [9] [10] , Pd(111) [11], Rh(100) [6], Ru(001) [12], Ni(100) [14], and Ni(110) [13]}. In these cases, the coadsorption of CO with another adsorbate results in the formation of new ordered surface structures different from those formed when either CO or the other adsorbate are present alone on these surfaces. The formation of these ordered, coadsorbed structures provides an excellent opportunity for studying the interaction between coadsorbed atoms and molecules under conditions where the relative geometry and stoichiometry can be established.

In this paper, we report that the CO induced ordering with several coadsorbates - sodium, benzene, fluorobenzene, and ethylidyne - on the Rh(111) crystal surface and the reduction in the C-O stretching frequency can be correlated with the surface dipole moments of the adsorbates. Here, the surface dipole moments are determined by measuring work function changes as a func-

tion of adsorbate coverages. We find that CO induced ordering occurs when CO is coadsorbed with an adsorbate that has a surface dipole moment oriented opposite to that of adsorbed CO, while disorder or segregation occurs when CO is coadsorbed with an adsorbate that has a similarly oriented dipole moment. We also find that NO, a ligand chemically similar to CO, has a surface dipole moment opposite that of ethylidyne when coadsorbed in the c(4x2) - NO + ethylidyne structure. Further, the magnitude of the reduction in the C-O stretching frequency appears to be directly related to the surface dipole moment of the coadsorbate.

Our laboratory has already reported several studies [1-5,7-9] for the individual CO coadsorption systems on the Rh(111) surface. For the various ordered structures observed, Table 1 lists the LEED structures, the unit cell size, the types and number of adsorbates per unit cell, and the C-O stretching frequency(ies) of the adsorbed CO molecules. Most of our information concerning the adsorbates within the ordered, coadsorbed structures has come from vibrational spectra obtained by high-resolution electron energy loss spectroscopy (HREELS). Figure 1 shows the vibrational spectra for four of the ordered structures where there is one CO molecule per coadsorbate. The vibrational spectra show that both CO and the coadsorbate maintain their molecular identity within the ordered, coadsorbed structures and are discussed in detail elsewhere [1,2,4,5].

For several of the CO coadsorbed structures [5] [8] , Van Hove and co-workers have determined by dynamical LEED analyses the adsorption geometries of the coadsorbed molecules including the bond lengths and bond angles. Table 1 also indicates the CO adsorption sites within the ordered structures, as determined by the LEED analyses. In all the CO coadsorbed structures on Rh(111) solved by LEED, the adsorption site of CO is an hcp hollow site, where one second layer rhodium atom sits below the three-fold site occupied by the CO molecule.

From Table 1 and Fig. 1, we see that C-O stretching frequency is greatly reduced from that of CO adsorbed alone on Rh(111) on either top or bridge sites and ranges from 1790 cm^{-1} for CO in the c(4x2)-CO + CCH_3 structure to 1410 cm^{-1} in the c(4x2)-CO + Na structure. If we assume that CO bonds at hollow sites in all of the coadsorbed structures, as borne out for those structures that have been determined by dynamical LEED analysis, then the 380 cm^{-1} spread of C-O stretching frequencies would indicate that interactions of varying strength occur between the CO molecule and the different coadsorbates. In principle, the Rh-CO stretching frequency should also provide information concerning the interaction between the coadsorbed molecules. Unfortunately, in our spectra, the Rh-CO stretching mode was either too weak to be observed or obscured by the vibrational modes of the coadsorbates.

In this paper, we discuss how the observed reduction in the C-O stretching frequency can arise from a combination of several interactions: (1) a vibrational

Stark effect from the electric field generated by neighboring dipoles, (2) charge transfer through the substrate into the $2\pi^*$ orbital of coadsorbed CO, and (3) direct chemical interactions between the coadsorbates. We also discuss the various interactions that can promote the formation of ordered, coadsorbed structures. As the work function measurements show that the coadsorbed molecules order when oppositely oriented dipoles are present in the unit cell, dipole-dipole interactions probably play a major role in the formation of coadsorbed structures. By using model calculations, we demonstrate that the dipole-dipole interaction energy between coadsorbate pairs ranges from -0.09 eV for the c(2√3x4)rect CO + C_6D_6 structure to -0.7 eV for the c(2x4) Na + CO structure on Rh(111).

2. Experimental

Our experiments were conducted in an ultra-high vacuum chamber equipped for low energy electron diffraction (LEED), Auger-electron spectroscopy (AES), thermal desorption spectroscopy (TDS), and high-resolution electron energy loss spectroscopy (HREELS). The HREEL spectrometer was used for both vibrational spectroscopy and work function measurements and has been described in detail elsewhere [15]. The sample was cleaned by cycles of Ar^+ sputtering, O_2 treatments, and annealing in vacuum at 1200 K. Surface cleanliness was monitored by Auger-electron spectroscopy and HREELS. During experiments, the background pressure in the chamber was typically $1x10^{-10}$ torr.

Figures 2a and b show schematically how we measure work function changes. The monochromator of the HREEL spectrometer provides a monoenergetic source of electrons (~10^{-10}A), which is focused onto the Rh(111) sample oriented perpendicular to the electron beam. The current to the sample is measured by a floating picoammeter connected in series with a bias voltage supplied by a DC ramp. When the bias voltage becomes sufficiently negative, the current to the sample drops to zero as the vacuum level of the sample is raised above the energy of the incident electrons. Since changes in the work function are also equal to the changes in the position of the vacuum level relative to the Fermi level, the change in work function is readily determined by measuring the shift in cutoff voltage from a plot of current versus bias voltage. Fig. 2c shows two such plots for the clean Rh(111) surface and for the Rh(111) surface covered with a quarter monolayer of sodium adatoms. Since the spread in energy of the electrons provided by the monochromator is small (~5 meV), the main inaccuracy comes from the shape of the current vs. voltage plot. (The high energy tail in the plot for the clean Rh(111) surface is from electrons hitting the sample supports as it is sensitive to the position of the sample but does not change as atoms and molecules are adsorbed or desorbed from the surface.) By this method, we are able to measure work function changes to within 0.01 eV.

3. Results

3.1 Work Function Measurements: Adsorption Alone

3.1.1 CO/Rh(111)

Figure 3 shows the work function change as a function of CO coverage on Rh(111). The coverage is defined as the ratio of adsorbed molecules per rhodium surface atoms. CO coverages were determined from the CO thermal desorption yield and calibrated against the $(\sqrt{3}x\sqrt{3})R30°$ LEED structure, which forms at 0.33 of a monolayer [16]. For CO coverages less than 0.33, where CO bonds only on top of the rhodium surface atoms [16] [17] , the work function change may be fit with a classical model for mobile adsorption. If we consider an well separated adsorbed species with surface density N, an initial dipole moment μ, and polarizability α, then the work function change ($\Delta\phi$) is given (in SI units) by [18]

$$\Delta\phi = \frac{-eN\mu}{\varepsilon_0[1 + (9/4\pi)\alpha N^{3/2}]}$$

where ε_0 is the vacuum permittivity. A good fit for $\theta_{CO.} \leq 0.33$ (shown by the dashed curve in Fig. 3 can be obtained with $\mu_{CO} = -0.67 \times 10^{-30}$ C•m (-0.2 D) and $\alpha_{CO} = 0.34 \times 10^{-28}$ m^3.

For $\theta_{CO} > 0.33$, $\Delta\phi$ increases dramatically until reaching a value of +1.05 eV at saturation coverage ($\theta_{CO} = 0.75$), where a (2x2) LEED pattern was observed. To achieve the (2x2) LEED structure, we found it necessary to cool the sample to 170 K, while the other CO coverages could be obtained at room temperature. For $\theta_{CO} > 0.33$, some of the adsorbed CO bonds bridging two rhodium atoms as well as on top sites [17] [19] . We attribute the dramatic increase in $\Delta\phi$ for $\theta_{CO} > 0.33$ to bridge bonded CO molecules on Rh(111) having a larger surface dipole

moment than top bonded CO. Since we are unable to determine the relative coverages of bridge and top bonded CO between 0.33 and 0.75 monolayer coverages, we are unable to model this system in order to determine the surface dipole moment or polarizability for bridge bonded CO on this surface.

3.1.2 Na/Rh(111)

Figure 4 shows the work function of the Rh(111) surface as a function of sodium coverage. The value of 5.4 eV for the work function of the clean Rh(111) surface is from Ref. [22]. Sodium coverages were determined from the sodium thermal desorption yield and calibrated against the $(\sqrt{3}x\sqrt{3})R30°$ and close-packed LEED structures [23]. Using the same model as for adsorbed CO, we deduce a surface dipole moment, μ_{Na}, of $+17 \times 10^{-30}$ C•m (+5.1 D), and a polarizability, α_{Na}, of 2.9×10^{-28} m^3 for low sodium coverages. Similar values have been observed for alkali adatoms on Rh(111) and other metal surfaces [20]. The dashed line in Fig. 4 shows that we can achieve a good fit for these values for $\theta < 0.4$. Above $\theta = 0.5$, the work function of the surface increases until reaching the value for sodium metal at just over the coverage needed to form one hexagonally close-packed monolayer.

3.1.3 Benzene and Fluorobenzene/ Rh(111)

Figure 5 shows the work function of the Rh(111) surface as a function of benzene and fluorobenzene exposure. The work function decrease of 1.36 eV for a saturation coverage of benzene on Rh(111) is in excellent agreement with the value of $\Delta\phi$ = -1.35 eV measured by Bertel et al., [22] using ultraviolet photoemission spectroscopy (UPS). For benzene adsorbed on Rh(111), we determined from the H_2 desorption yield that the benzene coverage is linear as a function of exposure up to saturation coverage. (Only a small fraction, < 10%, of benzene desorbs molecularly [24].) If we assume that the fluorobenzene is also linear as a function of exposure and using 0.17 and 0.16 for the saturation coverages of benzene [1] and fluorobenzene [4] , respectively, we can deduce, for benzene and fluorobenzene, surface dipole moments, μ_{ben} = +6.7 x 10^{-30} C•m (+2.0 D) and μ_{fb} = +6.5 x 10^{-30} C•m (+1.9 D), and polarizabilities, α_{ben} = 1.3 x 10^{28} m³ and α_{fb} = 1.5 x 10^{28} m³, respectively. It should be noted that the benzene-fluorobenzene values are within experimental error of each other. The difference in work function for the saturated layers of benzene and fluorobenzene is then attributed to the slight difference in saturation coverages.

3.1.4 Ethylidyne/ Rh(111)

Figure 6 shows the work function of the Rh(111) surface at 300 K as function of ethylene exposure. At this temperature ethylene decomposes to form ethylidyne ($\equiv CCH_3$) [21], which saturates at a coverage of 0.30 of a monolayer [25]. If we assume that the ethylidyne coverage is linear with ethylene exposure up to saturation coverage, then we find that μ_{eth} = +3.1 x 10^{-30} C•m (+0.9 D)

and $\alpha_{eth} = 0.62 \times 10^{-28}$ m³. If the ethylene sticking probability actually decreases with increasing coverage, as often occurs for adsorption processes, then μ_{eth} would be smaller than determined here.

3.2 Coadsorption of Similarly Oriented Dipoles

Table 2 lists the surface dipole moments and the polarizabilities of the adsorbates when adsorbed alone on the Rh(111) surface. Adsorbed CO has a negative surface dipole moment, while the other adsorbates, which all form ordered structures with coadsorbed CO, have positive surface dipole moments, opposite that of adsorbed CO. Therefore, it appears that CO-induced ordering occurs when CO is coadsorbed with an adsorbate with an oppositely oriented surface dipole moment.

To further test the hypothesis that ordering of coadsorbed molecules is driven by having oppositely oriented dipole moments within the ordered unit cells, we have coadsorbed molecules whose surface dipole moments are nominally oriented in the same direction and have found these combinations are disordered or segregated. Table 3 list these results. In these experiments, we tried to coadsorb the molecules at coverages and conditions similar to those where CO induced ordering of coadsorbed structures were observed. As discussed below, it appears that the dipole-dipole interaction energy promotes the formation of the coadsorbed structures for oppositely oriented dipoles but not for similarly oriented dipoles.

3.3 Work Function Measurements: Coadsorption with CO

We have also measured the work function for several of the ordered structures formed with coadsorbed CO on Rh(111). Table 4 lists the work functions observed for the structures formed by the organic adsorbates, both with and without coadsorbed CO. As can be seen from Table 4, the work function increases as the ratio of CO's to coadsorbates is increased, indicating that CO still has a negative surface dipole moment within the coadsorbed structures. Accurate determination of the dipole moments within the coadsorbed structures is difficult and would require detail measurements of work function changes as a function of coverage of both surface species. However, if we assume that benzene, fluorobenzene, and ethylidyne have the same surface dipole moment when coadsorbed with CO as when adsorbed alone on Rh(111), then we are able to estimate that CO has an effective surface dipole moment of ~ -2.4×10^{-30} C•m (-0.8 D) in the structures listed in Table 4. The assumption that benzene, fluorobenzene, and ethylidyne have the same dipole moments when coadsorbed with CO as when adsorbed alone is reasonable since previous HREELS studies [1] [2] [4] [5] indicate no significant changes in the adsorbate's internal structure when coadsorbed with CO.

We have also measured the work function change when NO, a ligand chemically similar to CO, is coadsorbed with a saturation coverage of ethylidyne. NO, like CO, forms a c(4x2) LEED structure on Rh(111) when coadsorbed with ethylidyne, but the ethylidyne species bonds at an hcp hollow site when

coadsorbed with NO rather than at the fcp hollow site it bonds at when adsorbed alone or with CO [5]. When NO is coadsorbed to form the c(4x2) structure, the work function increases by 0.45 eV, indicating that NO, like CO, has a negative dipole moment when coadsorbed with ethylidyne.

Figure 7 shows the work function of Rh(111) surface as a function of exposure to CO when the surface has been precovered with 0.15 and 0.25 of a monolayer of sodium. For both sodium coverages, the work function increases toward the clean metal value with increasing CO exposure, indicating that the CO still has a negative surface dipole moment when coadsorbed with sodium. For $\theta_{Na} = 0.25$, the initial dip in work function can be explained using a model developed by Albano [27]. This model shows that an initial dip in the work function can occur, due to cross depolarization effects, when a surface precovered with an adsorbate with a positive surface dipole moment is exposed to an adsorbate with a negative surface dipole moment. A dip occurs if the adsorbate with a positive surface dipole moment (i.e., Na) has a much larger polarizability than the adsorbate with a negative dipole moment (i.e., CO). In this case, the dipole moment of adsorbed CO induces, initially, an increase in the dipole moment of adsorbed Na larger than the dipole moment of the adsorbed CO, leading to an initial decrease in work function with the addition of CO.

4. Discussion

4.1 Interaction Energies

A necessary condition for the formation of intermixed, ordered structures when CO is coadsorbed with other adsorbates is that the Helmholtz free energy is less for the ordered structure compared to that of a disordered overlayer:

$$F_{ordered} - F_{disordered} = (U_{ordered} - U_{disordered}) - T(S_{ordered} - S_{disordered}) < 0$$

The difference in free energy, $\Delta F = F_{ordered} - F_{disordered}$, between an ordered and disordered overlayer is composed of two terms -- an entropy term, $T\Delta S = T(S_{ordered} - S_{disordered})$ that drives the system toward disorder and an interaction energy term, $\Delta U = U_{ordered} - U_{disordered}$ that drives the system toward order.

Our results indicate that the interaction energy, ΔU, favors ordered, coadsorbed systems when the coadsorbed molecules have oppositely oriented surface dipoles. In this section, we examine various possible contributions to the interaction energy between the coadsorbed molecules. First, we discuss the dipole-dipole interaction energy.

Obviously, oppositely oriented dipoles are attracted to each other, while similarly oriented dipoles repel each other. So, structures with oppositely oriented dipoles adjacent to each other are more energetically favorable than those with similarly oriented dipoles. To have a better feel for the magnitude of the dipole-dipole interaction energies of coadsorbed molecules, we have carried out model calculations for ordered arrays of dipoles to compute the dipole-dipole interaction energies for several of the ordered, coadsorbed structures on Rh(111), as well as the dipole electric fields normal to the surface within the unit cells. Here, we assume that CO has a dipole moment of -2.4×10^{-30} C•m, the esti-

mated value for coadsorbed CO, while the other coadsorbates are assumed to have the dipole moments measured when adsorbed alone on Rh(111). The results of these calculations are listed in Table 5 and the details of the calculations are discussed in the appendix. The negative sign for the interaction energy indicates that the coadsorbed structures are more energetically favorable, as one would expect for oppositely oriented dipoles. The dipole-dipole interaction energies range from -0.09 eV for the c(2√3x4)rect-CO + benzene structure to -0.7 eV for the c(4x2)-CO + Na structure. The CO + Na dipole-dipole interaction energy of 0.7 eV is comparable to the CO-Rh surface bond energy of 1.4 eV obtained from a thermal desorption measurement [28].

Norskov et al., [29] have theoretically investigated in more detail the dipole-dipole interaction of two coadsorbed species using effective medium theory to consider the effect the electrostatic potential induced by one adsorbate has on a neighboring adsorbate. These calculations take into account the rearrangement of charge between the adsorbates and the surface as well as the effect of screening of the electrostatic potential by the metal. They find, for example, that the interaction energy for CO and potassium coadsorbed on Fe(110) is in the range between 0.1 to 0.3 eV, smaller than the value of 0.7 eV that we estimate for Na and CO on Rh(111), probably because our calculations do not include screening effects.

It is reasonable to ask if any direct interactions (not through the substrate) occur between the coadsorbates other than dipole-dipole interactions. Other

types of direct interactions for most of the coadsorbed structures are unlikely except maybe for Van der Waals interactions, as the coadsorbed molecules are found to be separated by at least their Van der Waals dimensions in those cases where the structure has been determined by a dynamical LEED analysis [5] [8] . The Van der Waals interactions between closely packed adsorbed molecules, however, can be quite significant as shown by Gavezzotti et al., [30]. For example, these authors have calculated a Van der Waals packing energy of -0.12 eV per molecule (-2.7 kcal/mole) for benzene in a c(2√3x4)rect unit cell without coadsorbed CO, the same order as dipole-dipole interaction energies. A case where a strong, direct interaction may occur is for CO coadsorbed with Na in the c(4x2) structure. The very low C-O stretching frequency of 1410 cm^{-1} is less than the value of 1445 cm^{-1} observed for CO in the CO-alkali complex of potassium deltate, $K_2(CO)_3$ [31], suggesting that CO and Na may form a chemical complex on the surface. This possibility is discussed further in the next section on the vibrational frequencies of coadsorbed CO.

Next we comment on interactions occurring through the metal substrate. For CO adsorbed alone on Rh(111), Ruckenstein and Halachev [32] have calculated the energies of interactions mediated by the substrate for various separation distances. They find interaction energies of a few hundredths of an eV that are positive (repulsive) for small separation distances and negative (attractive) for intermediate distances. Within the coadsorbed, ordered structures, the CO molecules are separated by intermediate distances (4 to 8 Å), so the CO-CO inter-

actions should be attractive, which will further help to stabilize the ordered structures.

Another possible interaction, mediated by the metal surface, is charge transfer from one adsorbate to another through the substrate. Such an interaction has been widely discussed in the literature to occur between CO and alkali adatoms coadsorbed on metal surfaces [12] [33] [34] [35] . Here, the electropositive alkali adatom is thought to donate charge to the surface, which is then backdonated into the $2\pi^*$ orbital of adsorbed CO. It is tempting to suggest that the surface dipole moments measured in our experiments are related to the amount of charge transfer between the adsorbates and the surface. While this may be the case for an alkali atom, like sodium, adsorbed on a metal surface [36], the situation for the molecular adsorbates is more complex, since they can also have a dipole moment associated with their molecular structure, as well as one associated with charge transfer to the surface. As is discussed in the following section, however, the vibrational frequencies of coadsorbed CO indicate that some degree of charge transfer into the $2\pi^*$ orbital of CO occurs for several of the coadsorbed structures.

Finally, we should mention that the addition of CO to an adsorbed overlayer can also reduce the entropy of the system. The reduction in entropy comes about from CO blocking not only its own adsorption site, but, due to steric effects, also prevents coadsorbates from occupying neighboring sites. For example, CO when coadsorbed with benzene blocks a total of seven hcp hollow sites from benzene

adsorption on Rh(111). Since the sites blocked by an adsorbed CO become correlated with each other, the number of possible configurations for the coadsorbed system is reduced along with the entropy of a disordered overlayer, thereby making an ordered overlayer relatively more energetically favorable. Also, as the entropy for an intermixed overlayer is higher than for an segregated overlayer, the entropy helps promote intermixed structures over segregated structures. Even though entropy considerations help to explain why ordered, coadsorbed structures occur they do not account for only coadsorbed structures with oppositely oriented dipoles being observed, indicating that interaction energies play a dominant role.

4.2 C-O Stretching Frequency of Coadsorbed CO

The C-O stretching frequency can be a very sensitive indicator of the chemical environment of adsorbed CO. However, a shift in the C-O stretching frequency away from the gas phase value of 2145 cm^{-1} can originate from several different chemical and physical effects. Three distinct effects have been proposed and, in specific cases, demonstrated to be responsible for the reduction in the C-O stretching frequency of adsorbed CO: 1) a vibrational Stark effect where the reduction in frequency is proportional to the electric field at the CO molecule [37] [38] [39] [40] [41] [42] , 2) charge acceptance from the surface by the $2\pi^*$ orbital of adsorbed CO [12] [33] [34] [35] , and 3) the formation of a chemical complex between CO and neighboring adsorbates [43] [44] [45] [46] [47] . In this section, we show that the stretching frequency of coadsorbed CO

on Rh(111) is correlated to the surface dipole moment of the coadsorbates. We discuss this correlation in terms of various combinations of the three types of interactions.

The correlation between the C-O stretching frequency and the surface dipole moment of the coadsorbates can be seen most effectively by plotting the C-O stretching frequency vs. the dipole moment, as shown in Figure 8, for the coadsorbed, ordered structures where there is only one CO per coadsorbate. Even though only a few data points are available, it appears that the larger the surface dipole moment of the coadsorbate the lower the C-O stretching frequency of coadsorbed CO.

In order to see how the interactions that reduce the C-O stretching frequency can be related to the surface dipole moments, it is enlightening to compare the CO molecules in the c(4x2)-CO + CCH_3 and c(2√3x4)rect-CO + C_6D_6 structures. In both cases, the coadsorbed CO molecules have been determined by dynamical LEED analyses [5] [8] to be bonded at hcp hollow sites. In order to better understand how the interactions affect coadsorbed CO in these two structures, it would be important to know the C-O stretching frequency of CO bonded to a hollow site with no coadsorbates present. As CO does not bond to this site when adsorbed alone on Rh(111), the stretching frequency can not be determined, so we will estimate its value to be 1825 cm^{-1}, the same as CO bonded to a hollow site on the chemically similar Pd(111) surface [48] [49] . A check on this estimation can be made by extrapolating the results in Fig. 8 to a coadsorbate with

zero dipole moment. The extrapolation would predict a C-O stretching frequency of ~1840 cm^{-1}, close to the estimated value of 1825 cm^{-1}

For CO in the c(4x2)-CO + CCH_3 structure, a vibrational Stark effect is probably responsible for most of the decrease in the CO stretching frequency to 1790 cm^{-1}. For a vibrational Stark effect, the decrease in C-O stretching frequency is proportional to the electric field experienced by the CO oriented along its axis. The Stark tuning rate has been determined by Lambert for CO adsorbed on Ni(110) as 110±40 $cm^{-1}/V \cdot Å^{-1}$ [41] and on Ni(100) as 130 $cm^{-1}/V \cdot Å^{-1}$ [42]. Using the value for Ni(100) and our calculated value for the electric field of 0.23 V/Å, we calculate a Stark shift of 30 cm^{-1} for CO in the CO + CCH_3 structure. Adding the Stark shift to the observed frequency of 1790 cm^{-1} yields a value of 1820 cm^{-1}, close to the frequency of 1825 cm^{-1} estimated for CO adsorbed at a hollow site alone on Rh(111).

For CO in the c(2√3x4)rect-CO + C_6D_6 structure, the C-O stretching frequency, 1655 cm^{-1}, is shifted down ~190 cm^{-1} from the estimated frequency of CO bonded at a hollow site on Rh(111). As the calculated electric field at the CO when coadsorbed with benzene is similar to that when coadsorbed with ethylidyne, a Stark effect would only account for approximately 15 % of the 190 cm^{-1} reduction in stretching frequency. Within the c(2√3x4)rect structure, CO and benzene are separated by Van der Waals dimensions [8], so direct chemical interaction between coadsorbed CO and benzene is unlikely to be responsible for the observed reduction in the C-O stretching frequency. Therefore,

the most likely interaction reducing the C-O frequency is one mediated by the rhodium surface, such as charge donation to the surface by the benzene, which is then back donated into the $2\pi^*$ orbital of coadsorbed CO. The surface dipole moment, therefore, may be an indication of how much charge the benzene donates to the surface, which is then available to be accepted by the coadsorbed CO.

Now we discuss the two other points in Fig. 8, the c($\sqrt{3}$x4)rect-CO + C_6D_5F and c(4x2)-CO + Na structures. As C_6D_5F is chemically similar to C_6D_6, the reduction in the C-O stretching frequency for CO coadsorbed with fluorobenzene probably has the same origin as when coadsorbed with benzene, namely a small Stark effect plus an interaction mediated by the rhodium surface. For CO coadsorbed with Na in the c(4x2) structure, the C-O stretching frequency of 1410 cm^{-1} indicates a highly perturbed CO molecule within the unit cell. At the CO molecule, the electric field of 1.5 V/Å normal to the surface is fairly strong. Assuming a Stark tuning rate of 130 $cm^{-1}/V \cdot Å^{-1}$, we calculate a Stark shift of 200 cm^{-1} or about half the observed reduction from 1825 cm^{-1} to 1410 cm^{-1} The other half of the reduction in C-O stretching frequency presumably comes from charge transfer through the substrate or even possibly the formation of a CO-Na chemical complex. Several research groups [43] [44] [45] [46] [47] have proposed that CO and alkali adatoms form chemical complexes when coadsorbed on metal surfaces. Evidence for the formation of chemical complexes comes from the similarity of the low C-O stretching frequencies (1200 - 1600 cm^{-1}) observed for coadsorbed CO to those of polymeric CO anions in solid salts of alkali metals

with CO [43] [44] , and from ARUPS [45] [47] and XPS [46] results for CO coadsorbed with potassium on Cu(100), Ru(001), and Fe(100) that indicate that the $2\pi^*$ and 1π orbitals of CO are involved in a short range interaction with the coadsorbed potassium.

So the correlation shown in Fig. 8 that the larger the surface dipole moment of the coadsorbate the lower the C-O stretching frequency of coadsorbed CO appears to have a fairly complex origin. For CO coadsorbed with an adsorbate with a small surface dipole moment like ethylidyne, a Stark effect appears to be responsible for the small reduction in the stretching frequency. For CO coadsorbed with an adsorbate with a medium surface dipole moment, like benzene or fluorobenzene, other effects, such as possibly charge transfer through the surface, become important for reducing the C-O frequency. For CO coadsorbed with an adsorbate with a large surface dipole moment that indicates a large degree of interaction with the surface, all effects - Stark effects, charge transfer, and even chemical bonding between coadsorbates - become important in causing the large reduction observed in the C-O stretching frequency.

4.3 Comparison to Cluster Compounds

Often a surface chemical bond of molecular adsorbates can be thought as "cluster like" [50] [51] [52] - i.e., that the molecular bonding geometry and chemical interaction of molecular metal clusters can provide be a good model for the analogous surface chemical bond. For example, good agreement is observed

between the reported ν_{C-O} frequencies of CO bonded to one, two or three metal atoms in metal-carbonyl complexes and for CO chemisorbed with a similar bonding geometry on transition metal surfaces [53]. Consequently, it is interesting to see if CO coadsorption with other molecular adsorbates on Rh(111) can be compared with the analogous organometallic compounds - i.e., the substituted metal-carbonyl compounds with CO and other ligands bonded to the metallic center. As described in the previous sections, on a surface, the dipole-dipole interaction and interactions mediated by the substrate are the most common interactions between molecules coadsorbed on surfaces. However, in the substituted metal-carbonyl compounds, generally no significant direct interaction occurs between CO and the other molecular ligands, though a second order interaction between the ligands is usually observed to occur through the metallic center [51], which may be similar the substrate mediated interactions that occur on surfaces.

In substituted metal-carbonyl complexes, a charge transfer interaction between CO and other ligands is quite commonly observed, similar to the mechanism that appears to occur on metal surfaces. For the case of CO coadsorption with benzene or Na on Rh(111), we attribute part of the reduction in the C-O vibrational frequency to the charge transfer from benzene or sodium to the metal substrate, which then enhances the back donation to the $2\pi^*$ antibonding orbital of CO. In cluster complexes, both infrared spectroscopy and x-ray photoelectron spectroscopy (XPS) have been used to study how substituted ligands effect the degree of back donation to the $2\pi^*$ CO orbital [55] [56] . A shift in ν_{C-O} to lower

frequency and a corresponding lower force constant of the C-O bond are generally observed in the presence of π-electron donating ligands, which is attributed to charge transfer through the metallic center from the π-donating ligand to the $2\pi^*$ CO orbital [53] [54] . This lowering of the C-O force constant is seen for ligands like C_6H_6 and C_5H_5 in chromium and manganese carbonyl compounds [55]. Also, for a series of $RMn(CO)_5$ (R=ligand), the C-O force constant follows the sequence with ligand R: $C_3H_5 < CH_3 < H < I < Br < Cl < CF_3 < SiF_3$[55]. The difference here can be explained by the electron donating or withdrawing ability of each ligand; the better the electron donating group, the more the back bonding between the metallic center and CO. For similar ligands like CH_3 and CF_3, the "inductive effect" plays the most important role in making up the difference. When the better electron withdrawing atom (fluorine) substitutes for hydrogen in the methyl group, causing more electron withdrawing and less donating capability of CF_3 in comparison with CH_3. This is also a commonly observed phenomenon in organic chemistry. In our work, the slightly higher (1670 cm^{-1}) C-O frequency of CO when coadsorbed with C_6H_5F in comparison with 1655 cm^{-1} of CO coadsorbed with C_6H_6 in a c(2√3x4)rect structure, could be due to the "inductive effect" of the fluorine atom, similar to the effect observed between CF_3 and CH_3 in metal-carbonyl compounds. Consequently, it would be interesting to extend the present work to more highly fluorine substituted benzene to see if the trend to higher C-O frequency continues.

4.4 CO Induced Ordering on Other Surfaces

As mentioned at the beginning of this paper, CO induced ordering of adsorbates has been observed on several other metal surfaces besides Rh(111). To date, CO induced ordering has been observed for benzene on Pt(111) [1] [10] , Pd(111) [11], and Rh(100) [6] , for ethylidyne on Rh(100) [6], for potassium on Ru(001) [12] and Ni(110) [13] , and for hydrogen on Ni(100) [14]. Only for a few of these cases are work function measurements available. For benzene adsorbed on Pt(111), work function measurements by Gland and Somorjai [57] show that, for low benzene exposures, the work function decreases indicating that benzene on Pt(111) has a positive surface dipole moment. With increasing exposure of the Pt(111) surface to benzene, which in our experience is an effective way of introducing coadsorbed CO to form ordered, coadsorbed structures [1], Gland and Somorjai observed an increase in work function indicating that CO when coadsorbed with benzene on Pt(111) has a negative surface dipole moment. Other work function measurements done for adsorbates adsorbed alone on surfaces have shown the work function decreases for benzene adsorbed on Pd(111) [58] and Ni(111) [59] and for potassium on many metal surfaces [20], while when CO is adsorbed the work function generally increases [60]. Therefore, the results for CO induced ordering on other metal surfaces support in general the hypothesis that ordering occurs when oppositely oriented dipoles are coadsorbed.

5. Conclusions

To better understand the interactions responsible for CO induced ordering in many adsorbed overlayers, we have measured the changes in work function of

the Rh(111) surface when benzene, fluorobenzene, ethylidyne, sodium and CO are adsorbed, both alone and coadsorbed with CO. We find that CO induced ordering occurs when CO is coadsorbed with adsorbates that have an oppositely oriented surface dipole moment. Model calculations indicate that the attractive dipole-dipole interaction energy is largely responsible for the formation of ordered structures containing oppositely oriented dipoles.

We also find that the reduction in the C-O stretching frequency of coadsorbed CO correlates to the magnitude of the surface dipole moments of the coadsorbates. The reduction in the C-O stretching frequency is thought to originate from several effects: a Stark effect for CO coadsorbed with ethylidyne, charge transfer through the surface into the CO $2\pi^*$ orbital as well as a small Stark effect for CO coadsorbed with benzene and fluorobenzene, and a combination of a Stark effect, charge transfer, and even possibly the formation of a chemical complex for CO coadsorbed with sodium.

6. Acknowledgements

This work was supported by the Director, Office of Energy Research, Office of Basic Energy Sciences, Materials Sciences Division of the US. Department of Energy under contract No. DE-AC03-76SF00098. We are grateful for helpful discussions with Dr. M.A. Van Hove.

Appendix

In our model calculations, we first calculate, for an ordered array of dipoles, the electric fields normal to the surface at the two molecules within the unit cell, and then use the electric fields to determine the dipole-dipole interaction energies. We make the simplifying approximation that the dipole moments of the coadsorbed species can be treated by as point dipoles all lying in the same plane. Also, screening effects are neglected.

Consider two types of dipoles, A and B, coadsorbed in an order array and oriented perpendicular to the surface. Then the electric field normal to the surface at A from all the other dipoles is given by (in SI units)

$$\xi(A) = -\frac{1}{4\pi\varepsilon_0}\left[\mu'_A\sum\left(\frac{1}{r_{AA}}\right)^3_{ij} + \mu'_B\sum\left(\frac{1}{r_{AB}}\right)^3_{lk}\right]$$

where μ'_A and μ'_B are the apparent dipoles of A and B, r_{AA} and r_{AB} the distances between A and either the other A type dipoles or the B type dipoles, and the sums run over ether all the A dipoles or over all B dipoles. The apparent dipoles, μ'_A and μ'_B, are related to the effective dipoles by

$$\mu'_A = \mu_A + \alpha_A\xi(A)$$

and

$$\mu'_B = \mu_B + \alpha_A\xi(A)$$

If A and B occupy sites on identical lattices, but displaced from each other, then we can defined $\Sigma \equiv \Sigma \frac{1}{4\pi\varepsilon_0(r_{AA})^3_{ij}} = \Sigma \frac{1}{4\pi\varepsilon_0(r_{BB})^3_{ij}}$ and $\Sigma' \equiv \Sigma \frac{1}{4\pi\varepsilon_0(r_{AB})^3_{ik}} = \Sigma \frac{1}{4\pi\varepsilon_0(r_{BA})^3_{ik}}$. By solving for the electric field at the A dipole, one obtains

$$\xi(A) = \frac{\mu_A\Sigma + \mu_B\Sigma' + \mu_A\alpha_B[\Sigma^2 - (\Sigma')^2]}{\alpha_A\alpha_B[(\Sigma')^2 - \Sigma^2] - (\alpha_A + \alpha_B)\Sigma - 1]}$$

A similar expression can be derived for the electric field at a B dipole.

The dipole -dipole interaction energy for an A dipole and all the other dipoles is then given by

$$U_{dip}(A) = -\mu'_A\xi(A),$$

which we found during our calculations could be accurately approximated by

$$U_{dip}(A) = -\mu_A\xi(A).$$

In order to determine the net reduction or increase in energy due to the interaction of two types of dipoles, we have defined the interaction energies given in Table 5 to be the difference, per CO-coadsorbate pair, between the dipole-dipole interaction energy of the dipoles in a coadsorbed lattice and the case where the dipoles are in two separate lattices. For example, when CO and ethylidyne are coadsorbed in a c(4x2) lattice, U_{dip}(CO) = -0.034 eV and U_{dip}(eth) = -0.019 eV when coadsorbed, while U_{dip}(CO) = 0.026 eV and U_{dip}(eth) = 0.039 eV when adsorbed alone on a c(4x2) lattice. Consequently, the interaction en-

ergy between the different types of dipoles, as we have defined it, would be $(-0.34 - 0.019) - (0.026 + 0.039) = -0.012$ eV.

TABLE 1. CO-induced ordered structures on the Rh(111) surface.

Coadsorbate	LEED Structure*	No. of Rh surface atoms per unit cell	No. of coadsorbates per unit cell	No. of CO's per unit cell	C-O stretching frequency(ies) (cm^{-1})
--	$(\sqrt{3}x\sqrt{3})R30^\circ$	3	0	1	2010 (top)
--	(2x2)	4	0	3	2060 (top) 1855 (bridge)
ethylidyne ($\equiv CCH_3$)	c(4x2)	4	1	1	1790 (hcp hollow)#
propylidyne ($\equiv CCH_2CH_3$)	$(2\sqrt{3}x2\sqrt{3})R30^\circ$	12	3	1	1750
Acetylene (C_2H_2)	c(4x2)	4	1	1	1725
Fluorobenzene (C_6H_5F)	(3x3)	9	1	2	1720
	$c(2\sqrt{3}x4)$rect	8	1	1	1670
Benzene (C_6H_6)	(3x3)	9	1	2	1700 (hcp hollow)#
	$c(2\sqrt{3}x4)$rect	8	1	1	1655 (hcp hollow)#
Na	$(\sqrt{3}x7)$rect	14	4	7	1695
	c(4x2)	4	1	1	1410

*The notation (mxm) indicates a hexagonal unit cell with sides m times as long as the (1x1) unit cell sides; $R30^\circ$ means the unit cell is rotated 30° with respect to the (1x1) unit cell. The notation $(m\sqrt{3}xn)$rect indicates a rectangular unit cell with sides $m\sqrt{3}$ and n times as long as the (1x1) cell sides; the prefix "c" means the unit cell is a "centered" unit cell rather than a "primitive" unit cell.

#hcp hollow means one second layer metal atom lies below the three-fold hollow site, in contrast to a fcc hollow where no second layer atom lies below the three-fold site.

TABLE 2

Effective dipole moments, μ, and polarizability, α, for adsorbates alone on Rh(111).

Adsorbate	μ		α
CO (top site)	-0.67×10^{-30} C•m	(-0.2 D)	0.34×10^{-28} m^3
Na	+17	(+5.1)	2.9
C_6D_6	+ 6.7	(+2.0)	1.3
C_6D_5F	+ 6.5	(+1.9)	1.5
CCH_3	+ 3.1	(+0.9)	0.62

TABLE 3

Combinations of adsorbates with similarly oriented dipole coadsorbed on the Rh(111) surface.

Coadsorbates	LEED Patterns Observed
CO + NO	Disordered or compressed (2x2)-3CO [26]
Na + C_2H_2	Disordered
Na + $\equiv CCH_3$	Disordered
Na + C_6H_6	$(\sqrt{3}x\sqrt{3})R30^\circ$ + $(2\sqrt{3}x3)$rect*

*Since the $(\sqrt{3}x\sqrt{3})R30^\circ$ and $(2\sqrt{3}x3)$rect are observed for Na and benzene, respectively, adsorbed alone on Rh(111), the observation of a mixture of these two LEED structures implies that these two coadsorbates segregate on the surface.

TABLE 4

Work function of the Rh(111) surface at 310 K for various ordered structures, with and without coadsorbed CO. The work function of a bare Rh(111) surface is 5.4 eV [22].

Coadsorbate		Number of CO's per Coadsorbate		
		0	1	2
C_6D_6*	LEED Structure	(2√3x3)rect	c(2√3x4)rect	(3x3)
	Work Function (eV)	4.04	4.76	5.14
C_6D_5F*	LEED Structure	(√19x√19)R23.4°	c(2√3x4) rect	(3x3)
	Work Function (eV)	4.16	4.79	5.16
$\equiv CCH_3$	LEED Structure	disorder	c(4x2)	--
	Work Function (eV)	4.17	5.08	--

*The deuterated molecule was used in order to avoid interference from the background hydrogen in TDS measurements.

TABLE 5

Calculated electric fields and interaction energies for ordered arrays of dipoles.

Structure	Electric field at the CO (V/Å)	Electric field At the coadsorbate (V/Å)	Interaction energy (eV)
c(4x2)-CO+CCH_3	-0.23	0.098	-0.1
c(2√3x4)rect-CO+C_6D_6	-0.23	-0.46	-0.09
c(4x2)-CO+Na	-1.5	-0.56	-0.7

REFERENCES

1. C.M. Mate and G.A. Somorjai, Surface Sci. **160** (1985) 542.

2. C.M. Mate, B.E. Bent and G.A. Somorjai, J. Electron Spectrosc. Related Phenomena **39** (1986) 205.

3. C.M. Mate, C.-T. Kao, B.E. Bent and G.A. Somorjai, Surface Sci. **197** (1988) 183.

4. C.M. Mate, Ph.D. Thesis, University of California, Berkeley, 1986.

5. G.S. Blackman, C.-T. Kao, B.E. Bent, C.M. Mate, M.A. Van Hove and G.A. Somorjai, to be published.

6. B.E. Bent, C.-T. Kao, A. Slavin, and G.A. Somorjai, to be published.

7. B.E. Bent, C.M. Mate, J.E. Crowell, B.E. Koel and G.A. Somorjai, J. Phys. Chem. **91.** (1987) 1493.

8. M.A. Van Hove, R.F. Lin and G.A. Somorjai, J. Am. Chem. Soc **108** (1986) 2532; R.F. Lin, G.S. Blackman, M.A. Van Hove and G.A. Somorjai, Acta Crystallographia B43 (1987) 368.

9. M.A. Van Hove, R.F. Lin, D.F. Ogletree, G.S. Blackman, C.M. Mate and G.A. Somorjai, J. Vac. Sci. Technol. A **5** (1987) 692.

10. D.F. Ogletree, M.A. Van Hove and G.A. Somorjai, Surface Sci. **183** (1987) 1.

11. H. Ohtani, M.A. Van Hove and G.A. Somorjai, J. Phys. Chem., in press; H. Ohtani, B.E. Bent, C.M. Mate, M.A. Van Hove and G.A. Somorjai, Appl. Surf. Sci., in press.

12. R.A. dePaola, J. Hrbek, and F.M. Hoffmann, J. Chem. Phys. **82** (1985) 2484.

13. L.J. Whitman and W. Ho, J. Chem. Phys. **83** (1985) 4808.

14. L. Westerlund, L. Jonsson and S. Andersson, Surface Sci. **187** (1987) L669.

15. C.M. Mate, Ref. 4, Chapter 3;
the HREEL spectrometer is similar in design to the one described by H. Froitzheim, H. Ibach, and S. Lehwald, Rev. Sci. Instr. **46** (1975) 1325.

16. R.J. Koestner, M.A. Van Hove, and G.A. Somorjai, Surface Sci. **107** (1981) 439.

17. J.E. Crowell and G.A. Somorjai, Appl. Surface Sci. **19** (1984) 73.

18. J.R. MacDonald and C.A. Barlow, Jr., J. Chem. Phys. **39** (1963) 412; J.R. MacDonald and C.A. Barlow, Jr., J. Chem. Phys. **44** (1966) 202.

19. M.A. Van Hove, R.J. Koestner and G.A. Somorjai, Phys. Rev. Letters **50** (1983) 903.

20. A. Berko and F. Solymosi, Surface Sci. **187** (1987) 359, and references therein.

21. L.H. Dubois, D.G. Castner, and G.A. Somorjai, J. Chem. Phys. **72** (1980) 5234; B.E. Koel, B.E. Bent, and G.A. Somorjai, Surface Sci. **146** (1984) 179.

22. E. Bertel, G. Rosina and F.P. Netzer, Surface Sci. **172** (1986) L515.

23. H.W.K. Tom, C.M. Mate, X.D. Zhu, J.E. Crowell, Y.R. Shen and G.A. Somorjai, Surface Sci. **172** (1986) 466.

24. B.E. Koel, J.E. Crowell, C.M. Mate and G.A. Somorjai, J. Phys. Chem. **88** (1984) 1988.

25. B.E. Bent, unpublished results.

26. T.W. Root, G.B. Fisher and L.D. Schmidt, J.Chem. Phys. **85** (1986) 4687.

27. E.V. Albano, Appl. Surface Sci. **14** (1982-83) 183.

28. J.E. Crowell, Ph.D. Thesis, University of California, Berkeley, 1984, unpublished.

29. J.K. Norskov, S. Holloway and N.D. Lang, J.Vac. Sci. Technol. **A3** (1985) 1668; N.D. Lang, S. Holloway and J.K. Norskov, Surface Sci. **150** (1985) 24.

30. A. Gavezzotti, M. Simonetta, M.A. Van Hove and G.A. Somorjai, Surface Sci. **154** (1985) 109.

31. R. West, D. Eggerding, J. Perkins, D. Handy and E.C. Tuazon, J. Am. Cem. Soc. 101 (1979) 1710.

32. E. Ruckenstein and T. Halachev, Surface Sci. **122** (1982) 422.

33. M.E. Dry, T. Shingles, L.J. Boshoff and G.J. Oosthuizen, J. Catal. **15** (1969) 190.

34. E.L. Garfunkel, J.E. Crowell and G.A. Somorjai, J. Phys. Chem. **86** (1982) 310.

35. J. Lee, C.P. Hanrahan, J. Arias, R.M. Matin and H. Metiu, Phys. Rev. Letters **51** (1983) 1803.

36. D.L. Fehrs and R.E. Stichney, Surface Sci. **24** (1971) 309.

37. C.W. Bauschlicher, Jr., Chem. Phys. Letters **118** (1985) 307.

38. W. Muller and P. Bagus, J. Electron Spectrosc. Related Phenomena **30** (1983) 59.

39. P.S. Bagus, C.J. Nelin, W. Muller, M.R. Philpott, H. Seki, Phys. Rev. Letters **58** (1987) 559.

40. K. Kunimatsu, H. Seki, W.G. Golden, and M.R. Philpott, Langmuir **1** (1985) 245.

41. D.K. Lambert, Phys. Rev. Letters **50** (1983) 2106.

42. D.K. Lambert, J. Vac. Sci. Technol. **B3** (1985) 1479.

43. D. Lackey, M. Surman, S. Jacobs, S. Grider, and D.A. King, Surface Sci. **152/153** (1985) 513.

44. D. Lackey and D.A. King, J. Chem. Soc, Faraday Trans. 1, **83** (1987) 2001.

45. W. Eberhardt, F.M. Hoffmann, R. dePaola, D. Heskett, I. Strathy, and E.W. Plummer, and H.R. Moser, Phys. Rev. Letters **54** (1985) 1856; D. Heskett, E.W. Plummer, R.A. dePaola and W. Eberhardt, Phys. Rev. **B33** (1986) 5171.

46. J. Benziger and R.J. Madix, Surface Sci. **94** (1980) 119.

47. C. Somerton, C.F. McConville, D.P. Woodruff, D.E. Grider and N.V. Richardson, Surface Sci. **138** (1984) 31.

48. A.M. Bradshaw and F.M. Hoffmann, Surface Sci. **72** (1978) 513.

49. H. Ohtani, M.A. Van Hove and G.A. Somorjai, Surface Sci. **187** (1987) 372.

50. E.L. Muetterties, T.N. Rhodin, E. Band, C.F. Brucker and W.R. Pretzer, Chemical Reviews **79** (1979) 91.

51. M.R. Albert and J.T. Yates, Jr., The Surface Sientist's Guide to Organometallic Chemistry, American Chemical Society, Washington, D.C., 1987.

52. B.E. Bent and G.A. Somorjai, Progess in Colloid and Polymer Science **70** (1985) 38.

53. P.S. Braterman, Metal Carbonyl Spectra, Academic Press, London, 1975; R. Eischens and W.A. Pliskin, Advan. Catalysis **10** (1958) 1.

54. S.F.A. Kettle, Top. Curr. Chem. **71** (1977) 149.

55. S.C. Avanzino, A.A. Bakke, H.-W. Chen, C.J. Donahue, W.L. Jolly, T.H. Lee and A.J. Ricco., Inorg. Chem. **19** (1980) 1931.

56. W.L. Jolly, Top. Curr. Chem. **71** (1977) 149.

57. J.L. Gland and G.A. Somorjai, Surface Sci. **38** (1973) 157.

58. F.P. Netzer and J.U. Mack, J. Chem. Phys. **79** (1983) 1017.

59. J.E. Demuth and D.E. Eastman, Phys. Rev. Letters **32** (1974) 1123.

60. B.E. Nieuwenhuys, Surface Sci. **105** (1981) 505, and references therein.

FIGURE CAPTIONS

Fig. 1. Vibrational spectra obtained by HREELS for the ordered, coadsorbed structures on Rh(111) at 310 K where there is one CO molecule per coadsorbate.

Fig. 2. (a) Schematic diagram of the energy levels of the sample and the monochromator during work function measurements.

(b) Schematic diagram of the experimental set up for work function measurements.

(c) Typical current vs. bias voltage curves for the clean Rh(111) surface and a sodium covered Rh(111) surface. The shift in cutoff voltage gives the work function change.

Fig. 3. The work function change of the Rh(111) surface as a function of CO coverage. The dashed curve shows the fit with the model discussed in the text.

Fig. 4. The work function of the Rh(111) surface at 310 K as a function of sodium coverage. The clean Rh(111) work function is from Ref. [22]. The dashed curve shows the fit with the model discussed in the text.

Fig. 5. Work function of the Rh(111) surface at 300 K as a function of benzene and fluorobenzene exposure. The clean Rh(111) work function is from

ref. [22].

Fig. 6. Work function of the Rh(111) surface at 300 K as a function of ethylene exposure. The surface species responsible for the work function change is $\equiv CCH_3$ (ethylidyne). The clean Rh(111) work function is from Ref. [22].

Fig. 7. The work function of the Rh(111) surface at 310 K as a function of CO exposure when the surface was first precovered with θ_{Na} = 0.0, 0.15, and 0.25.

Fig. 8. The C-O stretching frequency in structures that have one CO per coadsorbate is plotted against the effective surface dipole moment of the coadsorbate when adsorbed alone on the Rh(111) surface.

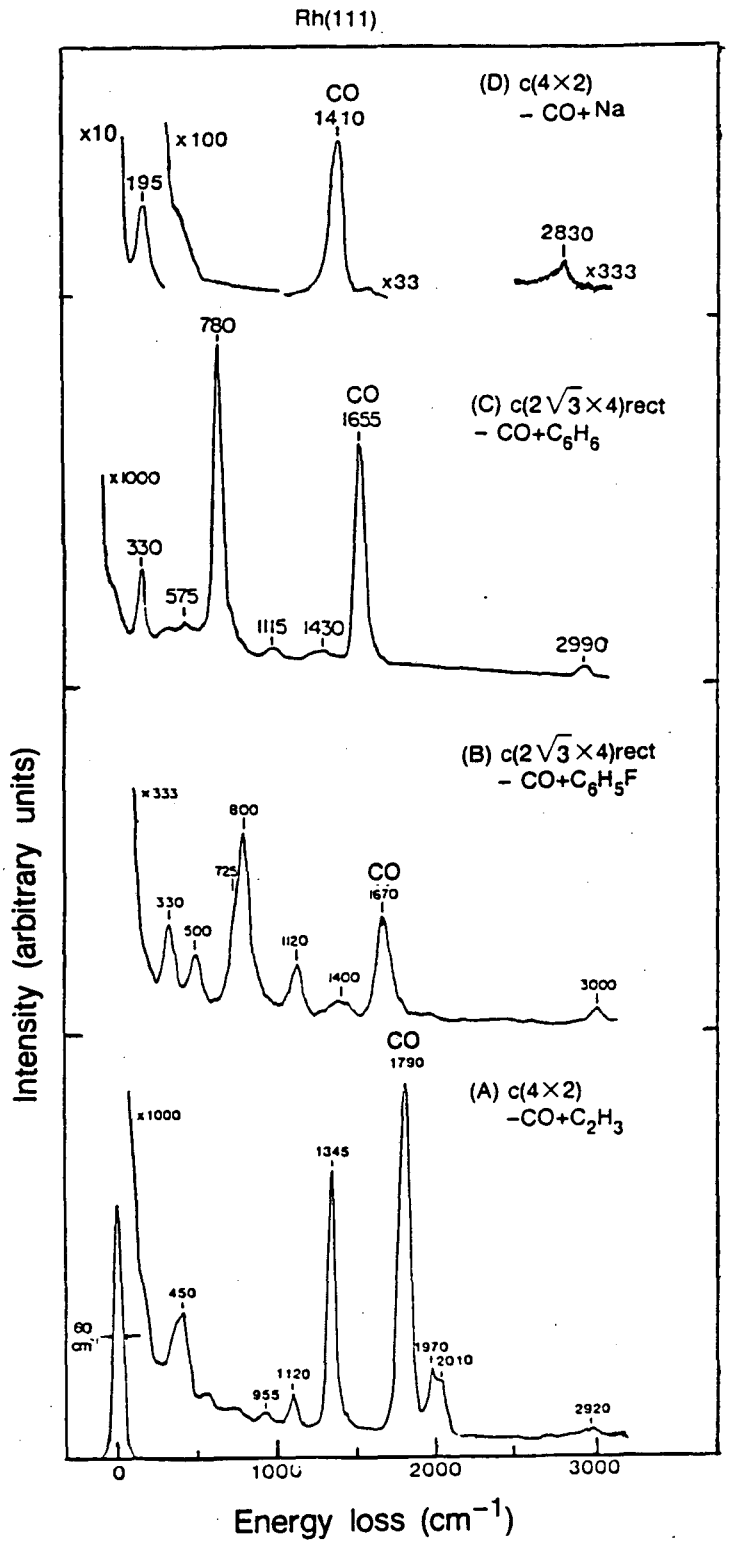

XBL 882-9564

Fig. 1

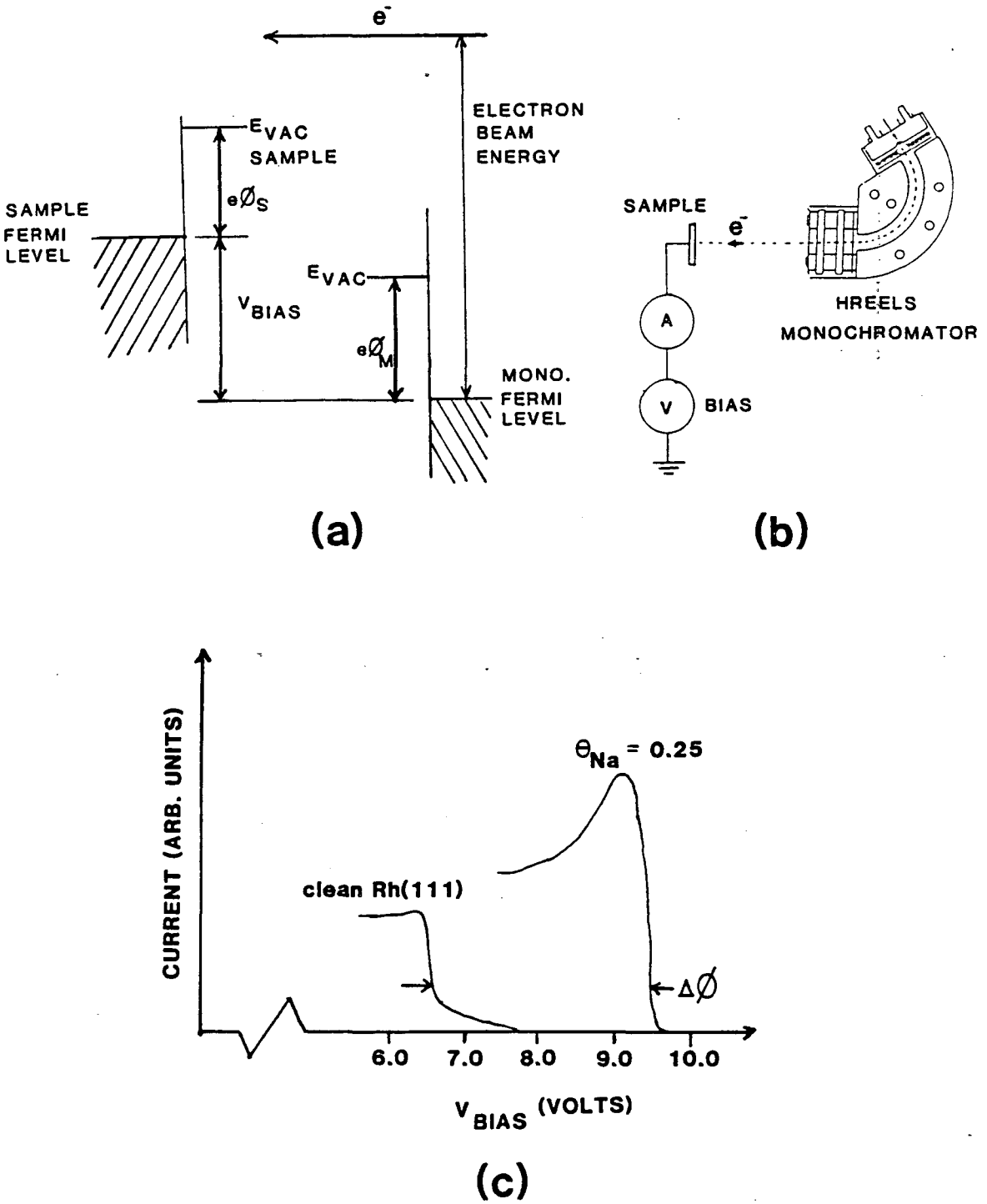

XBL 869-3420

Fig. 2

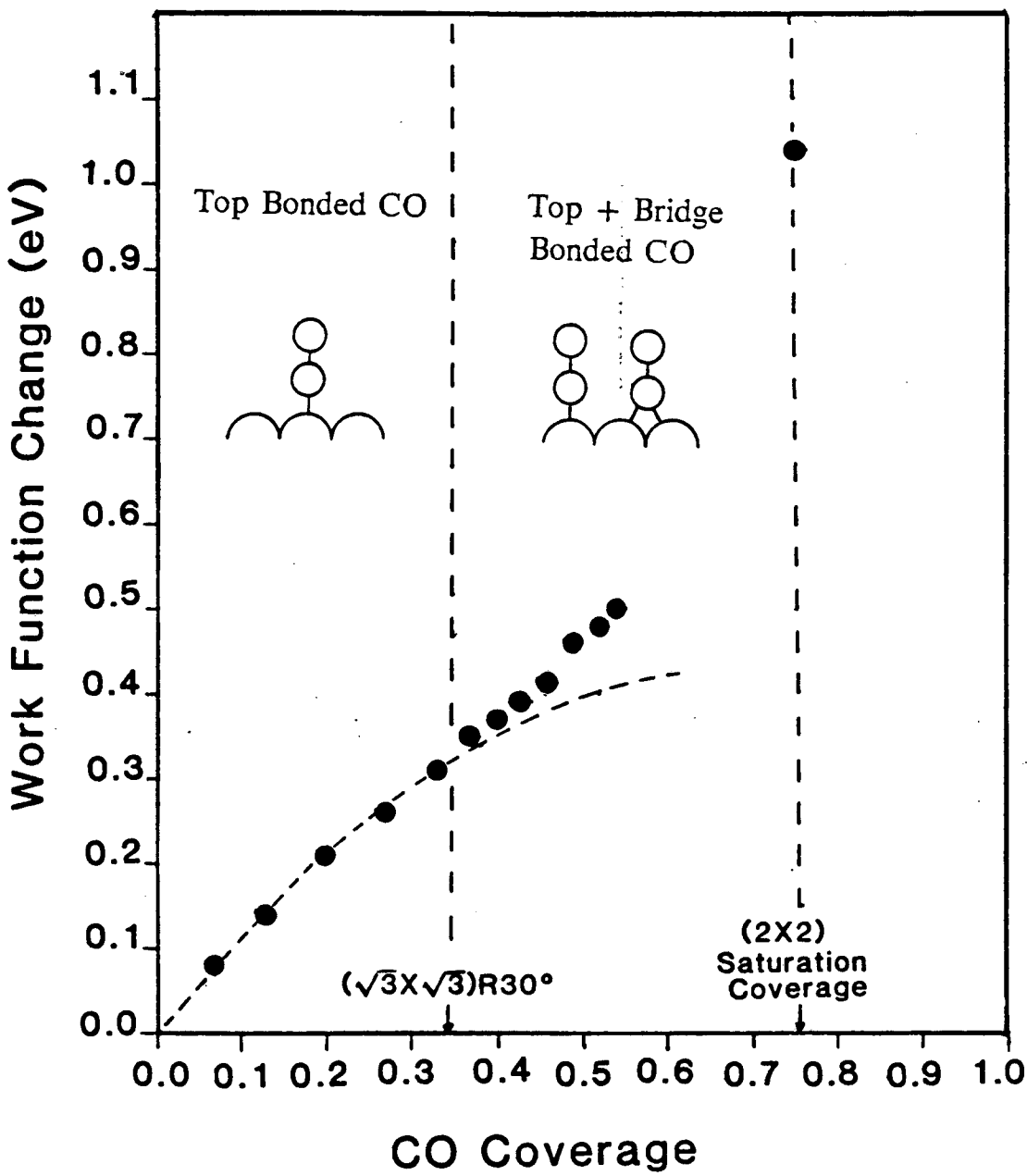

XBL 8610-3585A

Fig. 3

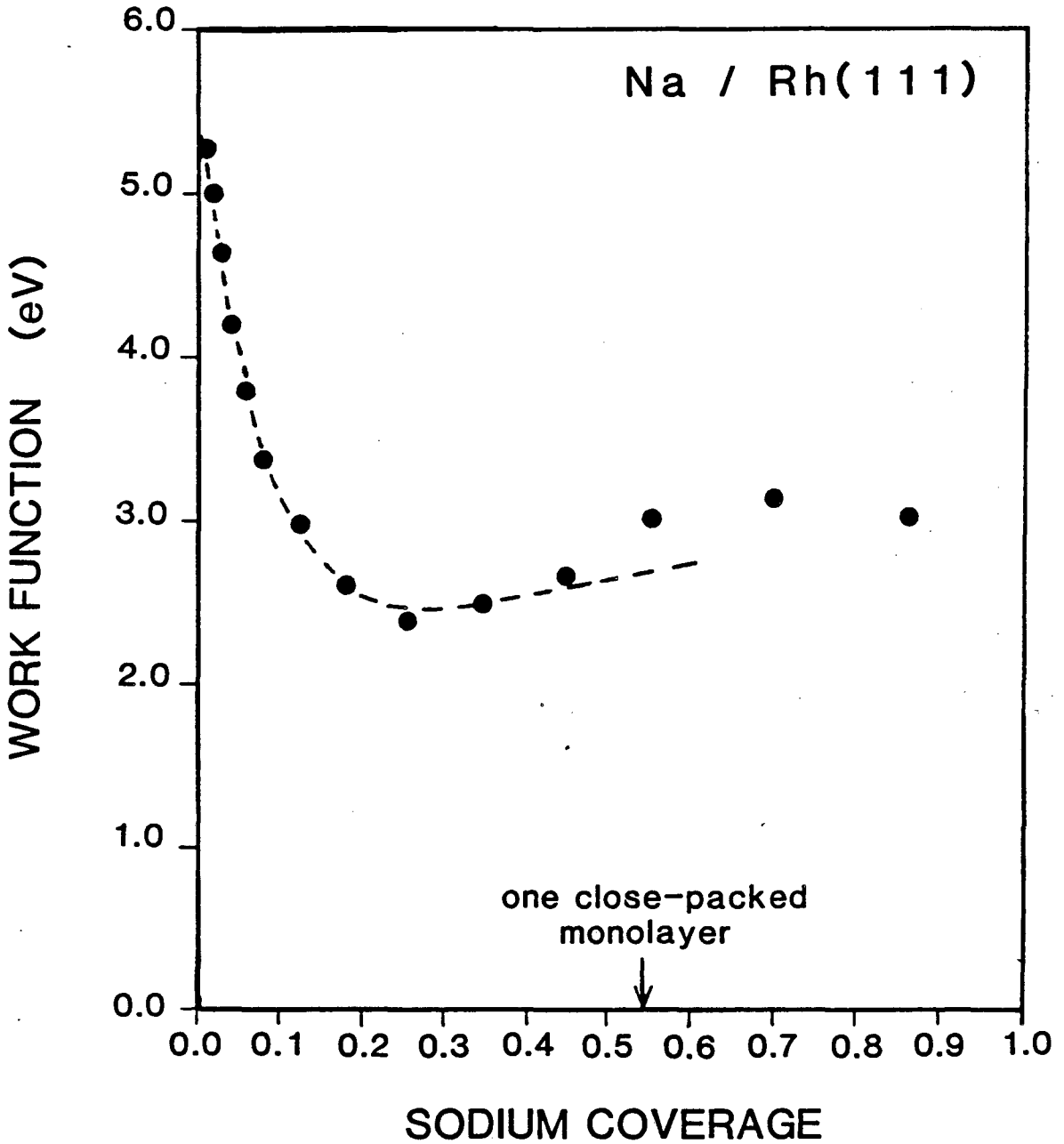

XBL 8610-3583A

Fig. 4

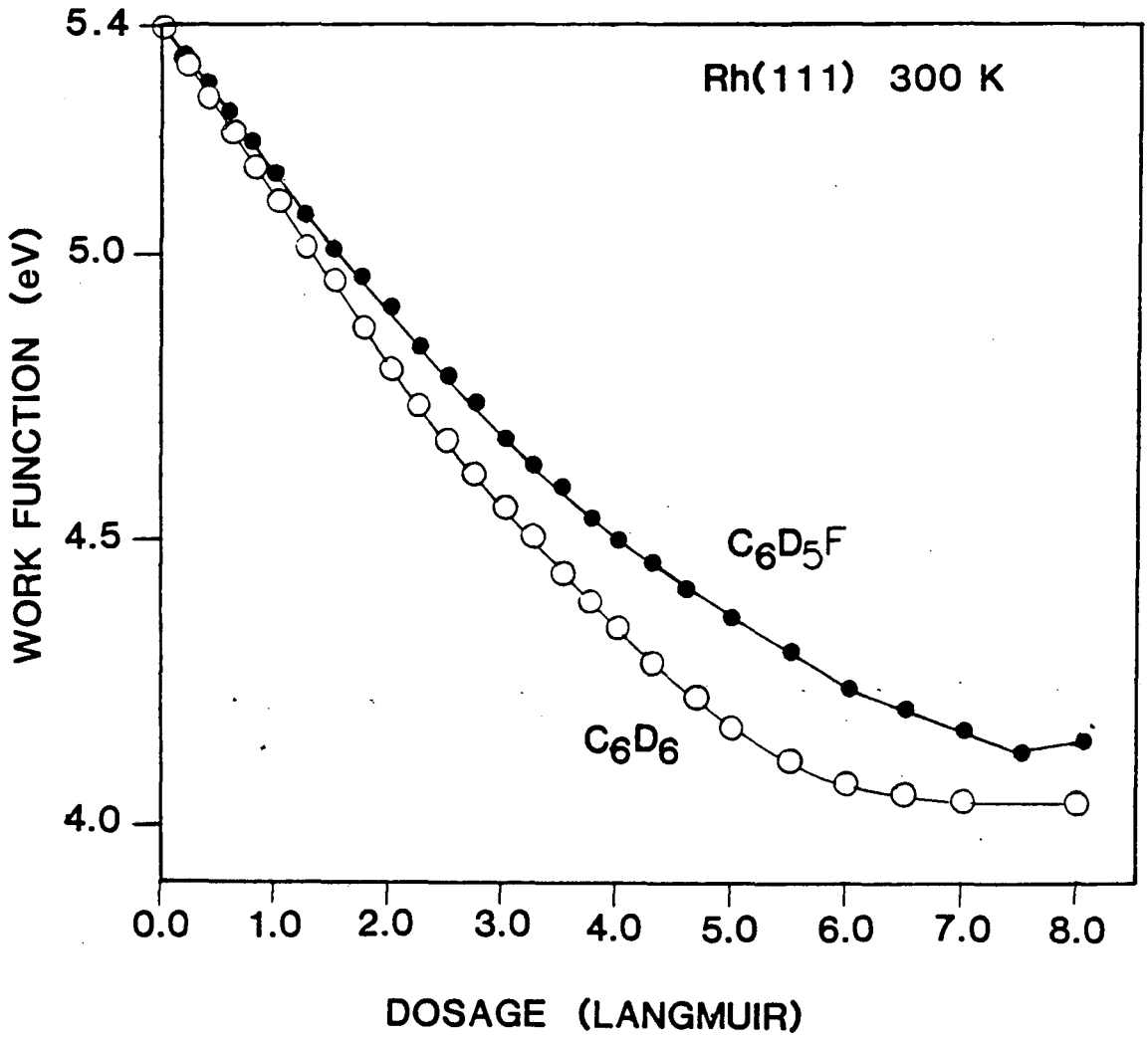

XBL 869-3581

Fig. 5

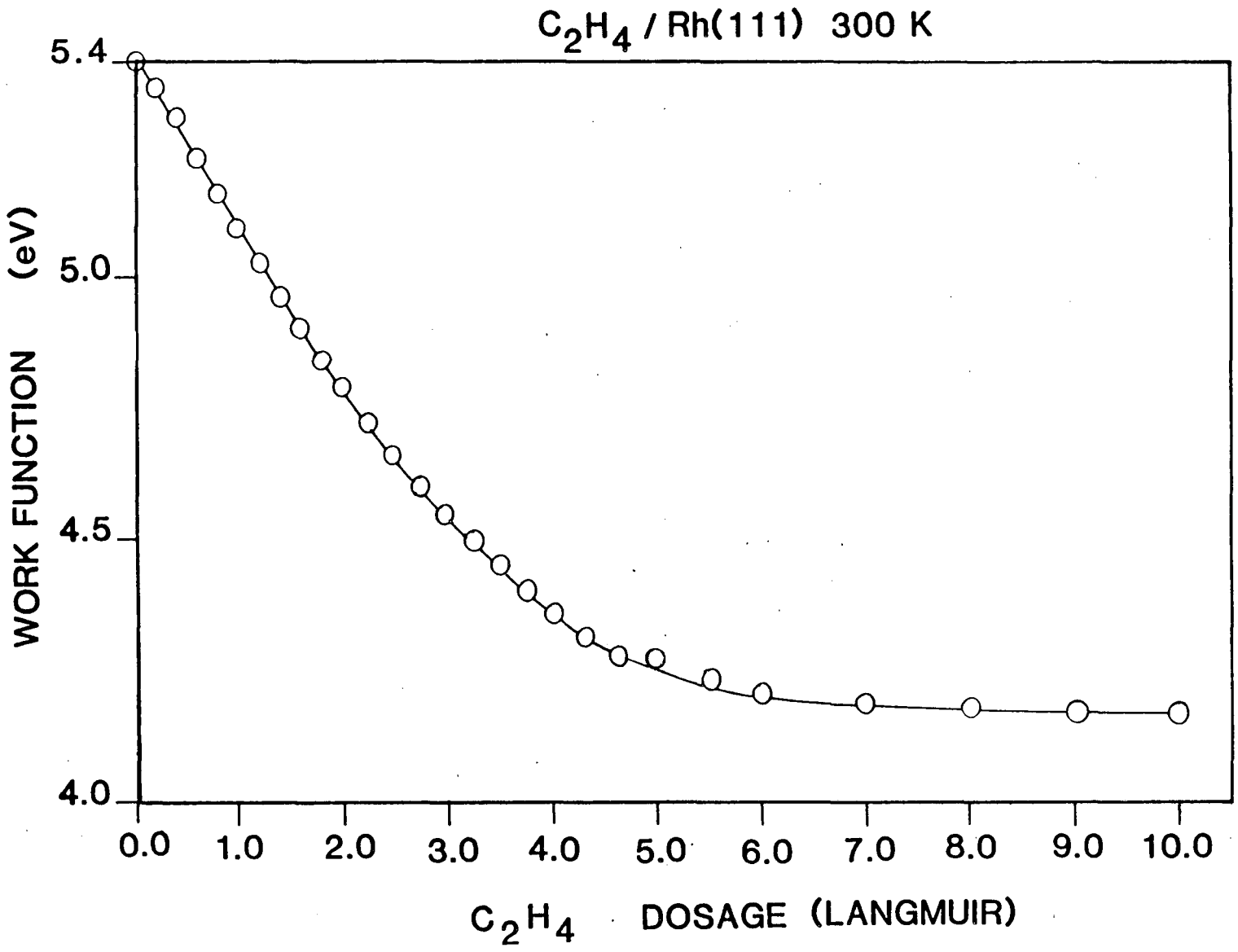

XBL 869-3580

Fig. 6

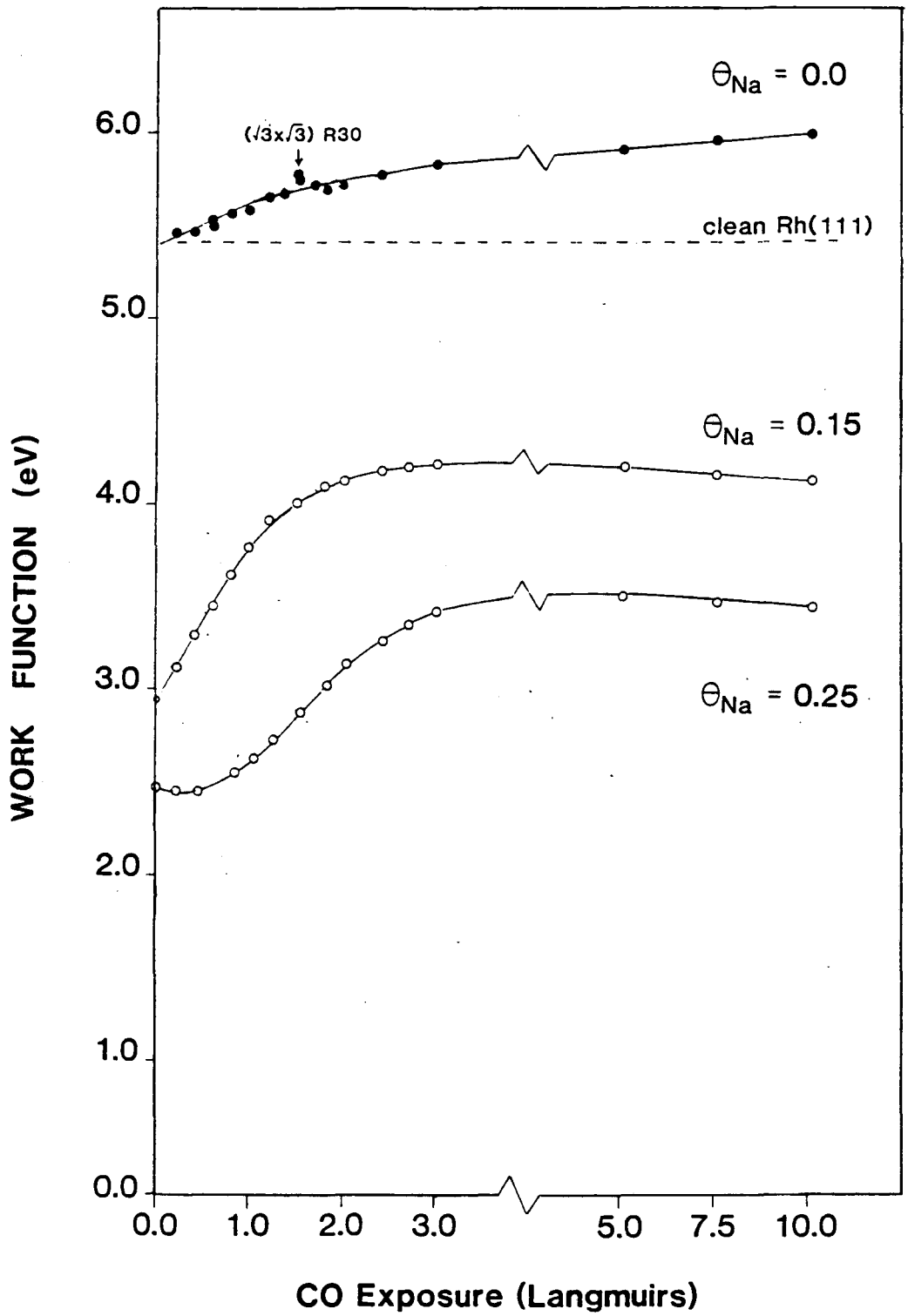

XBL 869-3435

Fig. 7

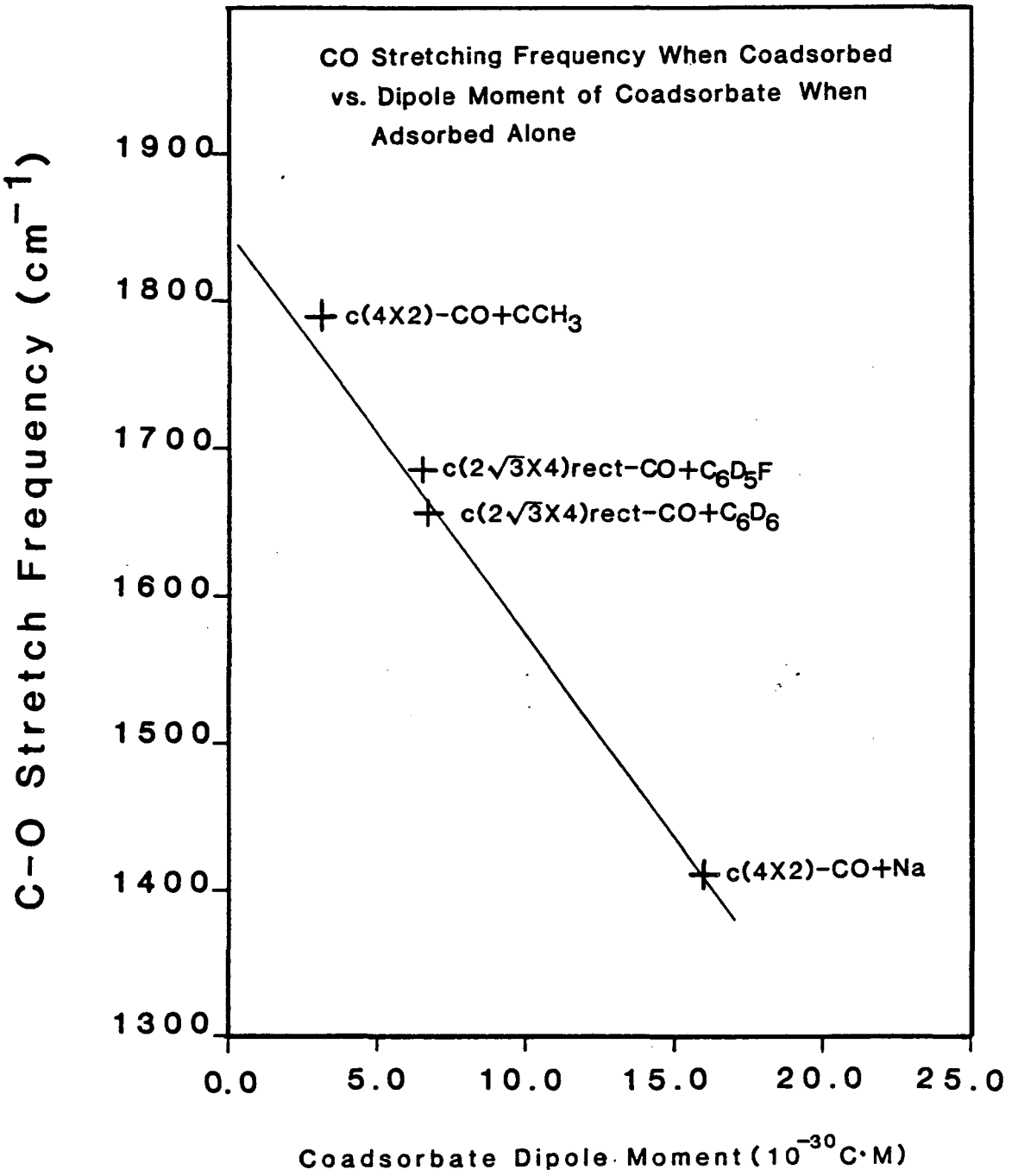

XBL 8610-3584

Fig. 8

LAWRENCE BERKELEY LABORATORY
TECHNICAL INFORMATION DEPARTMENT
UNIVERSITY OF CALIFORNIA
BERKELEY, CALIFORNIA 94720